

## SUMMARY OF DATA ON SECURE MULTIPLY IMAGED SYSTEMS

C.R. KEETON II AND C.S. KOCHANEK  
*Harvard-Smithsonian Center for Astrophysics*  
60 Garden Street, Cambridge, MA 02138, USA

**Abstract.** We present an extensive summary of the position, redshift, and flux data on the secure, multiply imaged, quasar and radio lenses. It includes neither the less-promising (in the opinion of the author) lens candidates nor the cluster lenses (which are too hard to reduce to short tables of numbers). A broader listing of suggested lenses and also of the cluster lenses is available at (see Pospieszalskia-Surdej et al. in this volume):  
[http://www.stsci.edu/ftp/stsci/library/grav\\_lens/grav\\_lens.html](http://www.stsci.edu/ftp/stsci/library/grav_lens/grav_lens.html)

### 1. Introduction

Table 1 lists the lenses and lens candidates discussed in this summary. The objects are sorted by a letter grade (A=“I’d bet my life this is a lens,” B=“I’d bet your life this is a lens,” and C=“You should worry if I’m betting your life.”) The B objects are almost certainly lenses, but are either very new candidates or double images missing a few too many observational checks. Some objects in C are certainly *not* lenses, because the C list contains all of the problematic wide separation double quasars, some of which are simply correlated quasars rather than lenses. Within each grade, the lenses are sorted in order of decreasing image separation or tangential critical radius.

Following Table 1 we present short data summaries for the individual objects, schematic diagrams or radio images, and time series of the flux ratios between the images where there is both data and space. We summarize only the data for the lenses (not models), and we do not attempt to give a complete list of all observational work on the object. References are only given for the data physically presented in the summaries, and

the summaries include only the most recent or most accurate observations. Whenever possible, we included error estimates for the data. *Please do not use this summary as your only reference for data on these lenses – the authors of the original papers deserve the credit for their work!*

**Acknowledgements:** We would like to thank E. Falco, J. Hewitt, D. Jones, J. Lehar, A. Patnaik, R. Porcas, K. Ratnatunga, and P. Schechter for their assistance in compiling this data and for commenting on the format.

Summary of Multiply Imaged Systems									
Name	G	$z_s$	$z_l$	$m_s$ mag	$m_l$ mag	$F_{\text{GHz}}$ mJy	$N_{im}$	$\Delta\theta$ "	Page
0957+561	A	1.41	0.36	16.7	18.5	$F_5 = 65.6$	(3)E	6.1	426
2016+112	A	3.27	(1.01)/(?)	$i=22.1$	$i=21.9$	$F_5 = 84.6$	(3)E	3.8	427
0142-100=UM673	A	2.72	0.49	16.8	19		2	2.2	424
PG 1115+080	A	1.72	0.29	15.8	20.2		4	2.2	428
MG 0414+0534	A	2.64		$I'=19.3$	$I'=21.1$	$F_5 = 977$	4E	2.1	429
CLASS 1608+656	A	1.39	0.63	(~20)	(~20)	$F_8 = 73.2$	4	2.1	430
MG 1131+045	A				(22)	$F_5 = 205$	2R	2.1	436
MG 1654+1346	A	1.74	0.25	$r=20.9$	$r=18.7$	$F_5 = 130.0$	R	2.1	436
B 1938+666	A			(23)		$F_5 = 316$	R	1.8	437
2237+0305	A	1.69	0.039	$B=16.8$	$B=15.6$	$F_8 = 0.336$	4	1.7	431
MG 1549+3047	A		0.11	23.3	16.7	$F_5 = 185$	R	1.7	437
B 1422+231	A	3.62	(0.65)	$r=15.6$	$r=21.8$	$F_5 = 557$	4E	1.3	432
H 1413+117	A	2.55		17.0		$F_8 \sim 0.1$	4	1.2	433
PKS 1830-211	A					$F_2 \sim 10^4$	2ER	1.0	438
MG 0751+2716	A		0.35		19	$F_5 = 202$	R	0.9	438
B 0218+357	A	(0.96)	0.68		$r=20.0$	$F_5 = 1209$	2ER	0.34	439
LBQS 1009-0252	B	2.74		$B=18.1$			2	1.5	424
CLASS 1600+434	B	1.61		~20		$F_8 = 132$	2	1.4	424
HST 14176+5226	B			$V=24.3$	$V=21.7$		4	1.4	434
HST 12531-2914	B			$V=25.5$	$V=23.8$		4	1.2	435
BRI 0952-0115	B	4.5					2	0.95	425
J03.13	B	2.55		17.1			2	0.84	425
1208+1011	B	3.80		$V=18.1$			2	0.48	425
2345+007	C	2.15		18.5	24.5		2	7.1	422
1120+019=UM425	C	1.47	(~0.6)	15.7			2	6.5	422
QJ 0240-343	C	1.4		$B=18.6$			2	6.1	422
1429-008	C	2.08		17.7			2	5.1	423
1634+267	C	1.96	(~0.6)	~19			2	3.8	423
HE 1104-1805	C	2.32		$B=16.9$			2	3.0	423

TABLE 1. The source and lens redshifts are  $z_s$  and  $z_l$ , the source and lens magnitudes are  $m_s$  and  $m_l$ , and the image separation or the diameter of the tangential critical line is  $\Delta\theta$ . The  $f$  GHz radio flux is given by  $F_f$ . Blank entries are unknown, and entries in parenthesis have low accuracy or substantial uncertainty. The magnitudes are  $R$  magnitudes unless otherwise specified. The number of compact images is  $N_{im}$ , an E indicates the images are extended, and an R indicates a ring.

2-image systems

Lens	Separation (")	Brightness	Redshift
2345+007	$\Delta\theta_{AB} = 7.06 \pm 0.01$ $(x, y)_A = (5.08, 2.90)$ $(x, y)_B = (-0.78, -1.04)$ $(x, y)_{G1} = (0.00, 0.00)$ Coordinates: A, $23^h 45^m 45.90^s$ , $+00^\circ 40' 40.4''$ (B1950)	$m_R(A) = 18.78 \pm 0.05$ $m_R(B) = 19.96 \pm 0.03$ $m_R(G1) = 24.5 \pm 0.5$	$z_s = 2.15$
1120+019 =UM425	$\Delta\alpha_{A-B} = 3.1 \pm 0.1$ $\Delta\delta_{A-B} = -5.7 \pm 0.1$ Coordinates: $11^h 20^m 46.7^s$ , $+01^\circ 54' 13.2''$ (B1950)	$m_R(A) = 15.7$ $m_R(B) = 20.1$ $m_R(B) - m_R(A) = 4.42 \pm 0.12$	$z_s = 1.465$   $(z_l \sim 0.6)$
QJ0240-343	$\Delta\theta = 6.1$	$m_B(A) = 19.00 \pm 0.05$ $m_B(B) = 19.77 \pm 0.05$	$z_s = 1.4$
Comments: The galaxy G1 is considered to be a lens candidate (F94). S91 find significant metal absorption systems at redshifts 1.4828 and 1.4912, as well as systems at 0.7545 (in component B only), 1.7717 (stronger in B than in A), 1.7977(A) and 1.7998(B), and 1.9832 (in A only). References: F94 (Fischer et al., 1994, ApJL, 431, L71); S91 (Steidel & Sargent, 1991, AJ, 102, 1610); W82 (Weedman et al., 1992, ApJL, 255, L5). Comments: The absolute magnitudes of A and B are uncertain by a couple of tenths of a magnitude because of the poorly determined zero point. $z_l$ is estimated by subtracting a scaled spectrum of A from the spectrum of B and interpreting the residuals as a galaxy. References: Meylan & Djorgovski, 1989, ApJL, 338, L1; Michalitsianos & Oliverson, 1995, ApJ, 439, 599. Comments: There is a metal-line absorption system at $z = 0.543$ , and a possible system at $z = 0.337$ . References: Tinney, these proceedings.			

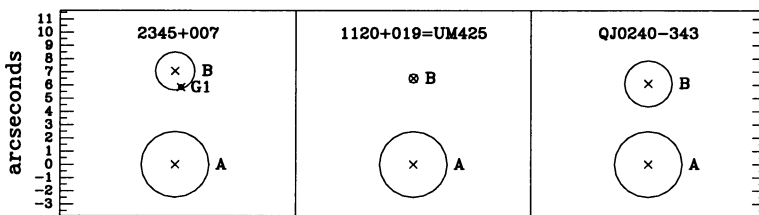


Figure 1. Schematic diagrams of 2-image systems. The orientation is arbitrary. The ratios of the circle areas are equal to the flux ratios. (The scale varies between Figs. 1-4.)

## 2-image systems

Lens	Separation (")	Brightness	Redshift
1429-008	$\Delta\theta = 5.14 \pm 0.10$	$m_R(A) = 17.74 \pm 0.05$ $m_R(B) = 20.77 \pm 0.10$	$z_s = 2.076$
Coordinates: A, $14^{\text{h}}29^{\text{m}}54.5^{\text{s}}$ , $-00^{\circ}53'04''$ (B1950)			
Comments: H89 find Mg II absorption systems at $z = 1.55$ and $z = 1.62$ . S95 find a Ly- $\alpha$ absorption line at $z = 1.662$ , as well as a C IV doublet at $z = 1.42$ with a velocity difference of 580 km/s between A and B.			
References: H89 (Hewett et al., 1989, ApJL, 346, L61); S95 (Smette et al., these proceedings).			
1634+267 <sup>†</sup>	$\Delta\alpha_{A-B} = 0.63$ $\Delta\delta_{A-B} = -3.72$	$m(A) = 19.15$ $m(B) = 20.75$	$z_s = 1.961$  ( $z_l \sim 0.57$ )
Coordinates: A, $16^{\text{h}}34^{\text{m}}59.1^{\text{s}}$ , $+26^{\circ}42'04''$ (B1950)			
Comments: ( <sup>†</sup> St91 suggest that this object's correct designation is 1634+267, not 1635+267.) In the spectrum of A, St91 find a metal absorption system at $z = 1.1262$ and a less-definite system at $z = 1.8389$ . T88 estimate $z_l$ by subtracting a scaled spectrum of B from the spectrum of A and interpreting the "excess flux" as a galaxy. St91 do not find evidence for "excess flux," but note that their 1" slit was smaller than T88's 2.5" slit.			
References: D84 (Djorgovski & Spinrad, 1984, ApJL, 282, L1); T88 (Turner et al., 1988, AJ, 96, 1682); Sr78 (Sramek & Weedman, 1978, ApJ, 221, 468); St91 (Steidel & Sargent, 1991, AJ, 102, 1610).			
HE 1104-1805	$\Delta\alpha_{A-B} = -2.7 \pm 0.1$ $\Delta\delta_{A-B} = 1.4 \pm 0.1$	$m_B(A) = 17.06 \pm 0.01$ $m_B(B) = 18.91 \pm 0.01$	$z_s = 2.319$
Coordinates: A, $11^{\text{h}}06^{\text{m}}33.45^{\text{s}}$ , $-18^{\circ}21'24.2''$ (J2000)			
Comments: A damped Ly- $\alpha$ plus metal absorption system is seen at $z = 1.66$ , and a Mg II absorption system is seen at $z = 1.32$ (only in A).			
References: Wisotzki et al., 1993, A&A, 278, L15; Wisotzki et al., 1995, A&A, 297, L59.			

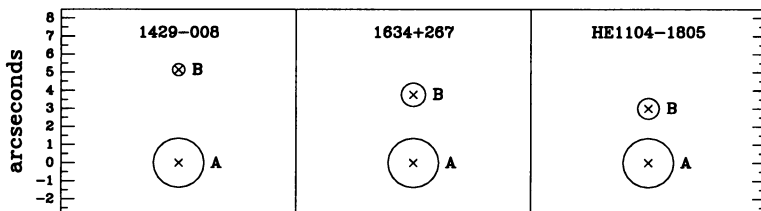


Figure 2. Schematic diagrams of 2-image systems. The orientation is arbitrary. The ratios of the circle areas are equal to the flux ratios. (The scale varies between Figs. 1-4.)

## 2-image systems

Lens	Separation (")	Brightness	Redshift
0142-100 =UM673	$\Delta\theta_{AB} = 2.22 \pm 0.03$ $\Delta\theta_{BG} = 0.8 \pm 0.2$ Coordinates: $01^{\text{h}}42^{\text{m}}48.6^{\text{s}}, -10^{\circ}00'13''$ (B1950)	$m_R(A) = 16.9 \pm 0.2$ $m_R(B) = 19.1 \pm 0.2$ $m_R(G) \approx 19$	$z_s = 2.719$ $z_l = 0.49$
LBQS 1009-0252	$\Delta\theta = 1.53 \pm 0.01$ $\Delta\alpha_{A-B} = 0.61$ $\Delta\delta_{A-B} = 1.41$ Coordinates: A, $10^{\text{h}}09^{\text{m}}43.97^{\text{s}}, -02^{\circ}52'12.0''$ (B1950)	$m_B(A) = 18.2$ $m_B(B) = 20.8$ $m_B(B) - m_B(A) = 2.52 \pm 0.20$	$z_s = 2.739$
CLASS 1600+434	$\Delta\theta = 1.39 \pm 0.01$ $\Delta\alpha_{A-B} = -0.72$ $\Delta\delta_{A-B} = 1.19$ Coordinates: A, $16^{\text{h}}01^{\text{m}}40.446^{\text{s}}, +43^{\circ}16'47.76''$ (J2000)	$F_{8.4\text{GHz}}(A) = 73$ mJy/beam $F_{8.4\text{GHz}}(B) = 56$ mJy/beam A/B = $1.30 \pm 0.04$	$z_s = 1.61$

Comments: G lies very nearly along the line joining A and B. It was identified by subtracting normalized spectra of A and B and matching the residual spectrum to the spectra of galaxies, and by noting the presence of faint absorption lines due to Ca II *H* and *K*. There is a high ionization absorption line system at  $z = 2.3564$ , a suspected Lyman absorption system at  $z = 2.7363$ , and a possible absorption line system at  $z = 1.8987$ .

References: MacAlpine & Feldman, 1982, ApJ, 261, 412; Surdej et al., 1987, Nature, 329, 695; Surdej et al., 1988, A&A, 198, 49.

Comments: The relative coordinates ( $\Delta\alpha_{A-B}$ ,  $\Delta\delta_{A-B}$ ) are taken from a figure caption in Hewett et al.; values given in a table are inconsistent with values given in the figure caption. A second quasar (labeled C) lies  $4.62''$  from image A and has  $m_B = 19.3$  and  $z = 1.627$ . Mg II absorption lines are seen at  $z = 0.8688$  and  $z = 1.6266$  in A and B; the  $z = 0.8688$  line is also seen weakly in C.

References: Hewett et al., 1994, AJ, 108, 1534; Surdej et al., 1993, Liège proceedings, p. 153.

References: Jackson et al., 1995, MNRAS, 274, L25.

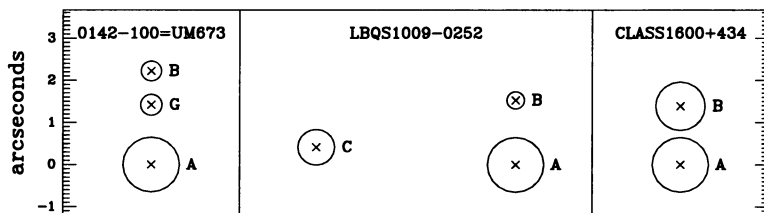


Figure 3. Schematic diagrams of 2-image systems. The orientation is arbitrary. The ratios of the circle areas are equal to the flux ratios. (The scale varies between Figs. 1-4.)

## 2-image systems

Lens	Separation (")	Brightness	Redshift
BRI 0952-0115	$\Delta\theta = 0.95$ Coordinates: $09^{\text{h}}52^{\text{m}}27.20^{\text{s}}$ , $-01^{\circ}15'53.0''$ (B1950) References: McMahon et al., 1992, Gemini, 36, 1.	$\Delta m = 1.35$	$z_s = 4.5$
J03.13	$\Delta\theta = 0.84 \pm 0.02$ Comments: There are absorption line systems at $z = 2.34$ (Ly- $\alpha$ and C IV) and $z = 1.085$ (metal). References: Claeskens et al., these proceedings.	$m_R(\text{A}) = 17.2 \pm 0.1$ $m_R(\text{B}) = 19.3 \pm 0.1$ $m_R(\text{B}) - m_R(\text{A}) = 2.14 \pm 0.05$	$z_s = 2.55$
1208+1011	$\Delta\theta = 0.476 \pm 0.004$ Coordinates: $12^{\text{h}}08^{\text{m}}23.73^{\text{s}}$ , $+10^{\circ}11'07.9''$ (B1950) Comments: Magnitude uncertainties are not stated. The flux ratio is from aperture photometry in the F555W (V) band; the uncertainty represents scatter in the measurements. Measurements in other bands (F439W, F702W, F785LP) also yield a flux ratio of approximately 4:1. References: Bahcall et al., 1992, ApJL, 392, L1; Bahcall et al., 1992, ApJL, 400, L51; Hazard et al., 1987, Nature, 322, 38; Magain et al., 1992, A&A, 253, L13.	$m_V(\text{A}) \approx 18.3$ $m_V(\text{B}) \approx 19.8$ A/B = $4.2 \pm 0.1$	$z_s = 3.803$

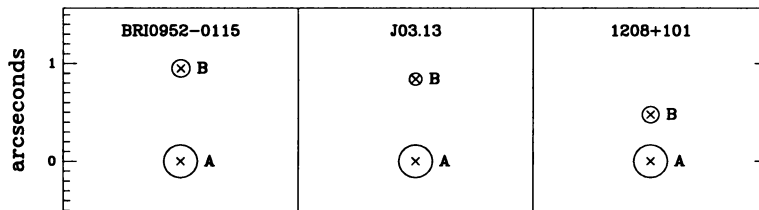


Figure 4. Schematic diagrams of 2-image systems. The orientation is arbitrary. The ratios of the circle areas are equal to the flux ratios. (The scale varies between Figs. 1-4.)

0957+561 (A: 09<sup>h</sup>57<sup>m</sup>57.324<sup>s</sup>, +56°08'22.344" [B1950; Go84])

	$-\Delta\alpha$ (")	$\Delta\delta$ (")	$F_{\text{GHz}}$ (mJy)	Jet Length (mas)	Jet PA (°)
A	$1.25252 \pm 0.00003$	$6.04662 \pm 0.00004$	$F_5 = 35.9 \pm 0.2$	$48.3 \pm 0.1$	$19.9 \pm 0.1$
B	0.0	0.0	$F_5 = 27.2 \pm 0.1$	$58.8 \pm 0.1$	$17.8 \pm 0.1$
G'	$-0.181 \pm 0.001$	$1.029 \pm 0.001$	$F_2 = 0.6 \pm 0.1$		
G/G1	$-0.19 \pm 0.03$	$1.00 \pm 0.03$	$F_5 = 2.50 \pm 0.09$		

Positions and fluxes (left): The position of A is from Go84. The position of the third VLBI component G' is from Go83. The position of the optical galaxy G1 is from S80. The fluxes of A, B, and G are from Ro85, and the flux of G' is from Go83.

Jet orientation (right; Ga94): The core-jet configuration is modeled with 6 Gaussian components; the lengths and position angles given here are for the most luminous components (A<sub>5</sub>, B<sub>5</sub>). Data from VLBI observations, 1989 Nov 8.

Transformation matrix (Ga94): The transformation matrix  $M^{BA}$  is specified by its eigenvalues ( $M_i$ ), the position angles of its eigenvectors ( $\phi_i$ ), and the spatial derivative of the eigenvalues along the direction of the jet ( $\dot{M}_i$ ). ( $\phi_i \equiv 0$  by assumption.)

$M_1$	$=$	$1.23 \pm 0.04$	$M_2$	$=$	$-0.50 \pm 0.03$
$\phi_1$	$=$	$18.6^\circ \pm 0.1^\circ$	$\phi_2$	$=$	$118^\circ \pm 6^\circ$
$\dot{M}_1$	$=$	$(0.5 \pm 1.5) \times 10^{-3} \text{ mas}^{-1}$	$\dot{M}_2$	$=$	$(2.6 \pm 0.8) \times 10^{-3} \text{ mas}^{-1}$

Lens velocity dispersion:  $\sigma = 303 \pm 50 \text{ km/s}$  (Rh91).

References: Ga94 (Garrett et al., 1994, MNRAS, 270, 457), Go83 (Gorenstein et al., 1983, Science, 219, 54), Go84 (Gorenstein et al., 1984, ApJ, 287, 538), P95 (Porcas et al., these proceedings), Rh91 (Rhee, 1991, Nature, 350, 211), Ro85 (Roberts et al., 1985, ApJ, 293, 356), and S80 (Stockton, 1980, ApJL, 242, L141).

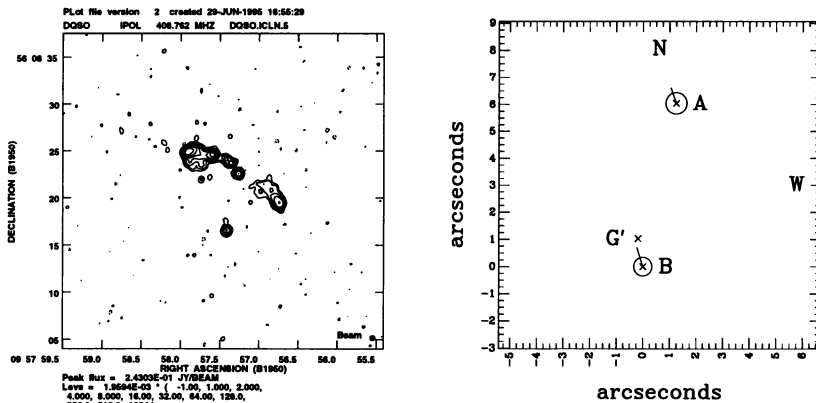


Figure 5. Left: 408 MHz MERLIN map of 0957+561, from P95. Right: Schematic diagram of 0957+561. (The scale differs from the MERLIN map.) The ratio of the circle areas is equal to the core flux ratio ( $0.75 \pm 0.02$ , Ga94). The lines give the direction of the jets, and the ratio of the line lengths is equal to the ratio of the jet lengths.

2016+112 (A:  $20^{\text{h}}16^{\text{m}}55.4790^{\text{s}}$ ,  $+11^{\circ}17'46.537''$  [B1950; G94])

ID	$-\Delta\alpha$ "	$\Delta\delta$ "	$F_{5\text{GHz}}$ mJy	$-\Delta\alpha$ "	$\Delta\delta$ "	$\lambda 5180$ mag( $\pm$ mag)	$g$ mag( $\pm$ mag)	Object
A	0.000	0.000	15.8	0.00	0.00	20.95(0.02)	22.72(0.03)	QSO image
B	3.009	-1.489	17.2	3.02	-1.49	21.48(0.02)	23.09(0.03)	QSO image
$C_2/C'$	2.188	-3.205	4.4	2.03	-3.37	22.85(0.08)	24.39(0.12)	QSO image
$C_1/C$	2.077	-3.220	47.2	2.09	-3.21			Radio galaxy?
D				1.68	-1.95			Galaxy
A1				2.9	2.0	22.8 (0.2)		Gas cloud
B1				5.8	-1.2	22.8 (0.2)		Gas cloud

G94 data (left):  $C_1$  and  $C_2$  denote two radio sources resolved in this map. The uncertainties in the relative positions are  $\leq 5$  mas. The map has an rms noise of  $75 \mu\text{Jy}/\text{beam}$ . Data from 5GHz MERLIN observations, 1992 July 11-12.

S86 data (right): C denotes a radio source, and  $C'$  denotes a source identified via a Ly- $\alpha$  emission line.  $\lambda 5180$  denotes a filter centered at  $5180 \text{ \AA}$  with FWHM  $100 \text{ \AA}$ . The uncertainties in the positions are  $0.1''$  for A, B, and  $C'$ ;  $0.3''$  for A1 and B1;  $0.01''$  for C (from a VLA map); and  $0.1''$  for D (from  $i$ -band observation in S85). The uncertainty given for the magnitudes is photon noise. Data from the Hale telescope, 1985 Oct 13.

Miscellaneous: A, B,  $C'$ , A1, and B1 are identified via a Ly- $\alpha$  emission line at  $5193 \text{ \AA}$  (S86); A1 and B1 are thought to be two gas clouds located near the lensed QSO and are thought to be magnified but not multiply imaged (S87). Though the radio source  $C/C_1$  was thought to be a galaxy, new observations that resolve it into three subcomponents question this interpretation (G95).

References: G94 (Garrett et al., 1994, MNRAS, 269, 902), G95 (Garrett et al., these proceedings), S85 (Schneider et al., 1985, ApJ, 294, 66), S86 (Schneider et al., 1986, AJ, 91, 991), and S87 (Schneider et al., 1987, AJ, 94, 12).

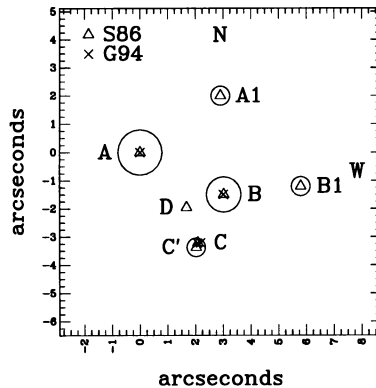


Figure 6. Positions from G94 ( $\times$ ) and S86 ( $\Delta$ ). The ratios of the circle areas are equal to the  $\lambda 5180$  flux ratios from S86.

PG 1115+080 ( $11^{\text{h}}15^{\text{m}}41.5^{\text{s}}$ ,  $+08^{\circ}02'24''$  [B1950; W80])

ID	<i>x</i> "	<i>y</i> "	<i>V</i> mag	<i>I</i> mag	<i>x</i> "	<i>y</i> "	<i>V</i> mag	<i>B</i> mag	<i>R</i> mag
A1	-1.294	-2.036	16.90	16.12	-1.27	-2.08	16.99	17.48	16.71
A2	-1.448	-1.582	17.35	16.51	-1.44	-1.62	17.27	17.74	16.95
B	0.362	-1.949	18.87	18.08	0.39	-1.95	18.74	19.19	18.46
C	0.000	0.000	18.37	17.58	0.00	0.00	18.26	18.71	17.97
G	-0.355	-1.322		18.36	-0.33	-1.35	20.89	> 21.6	20.20

K93 data (left): *x* is approximately west, *y* is approximately north. The internal position uncertainties are 5 mas for the quasar images and 50 mas for the galaxy. The relative fluxes are uncertain by 1.5% in *I* (F785LP) and 3% in *V* (F555W), but the zero-point for magnitudes is uncertain by 0.3 mag. Data from HST WFPC, 1991 Mar 3.

C87 data (right): *x* is approximately west, *y* is approximately north. The position uncertainties are not clearly stated, but separate reductions of *B*, *V*, and *R* frames agreed within an rms difference of 4 mas. Magnitude uncertainties for the quasar images are 0.03 in *V* and 0.05 in *B* - *V* and *V* - *R*; magnitude uncertainties for the galaxy are 0.05 in *R* and 0.1 in *V* - *R*. Galaxy magnitudes determined with a 1.6" diameter aperture. Data from CFHT, 1986 Feb 19.

References: C87 (Christian et al., 1987, ApJ, 312, 45), K93 (Kristian et al., 1993, AJ, 106, 1330), S93 (Schechter, 1993, Liège Proceedings, p. 119), V86 (Vanderriest et al., 1986, A&A, 158, L5), and W80 (Weymann et al., 1980, Nature, 285, 641).

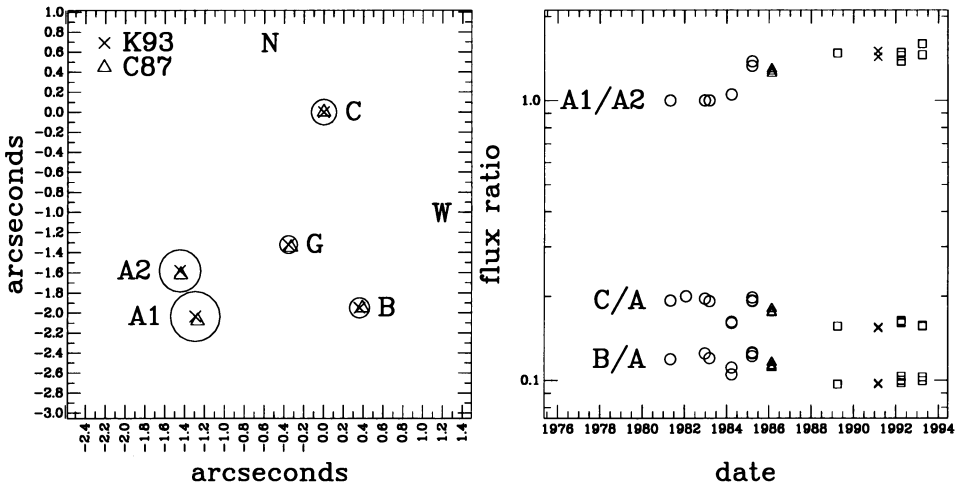


Figure 7. Left: Positions from K93 (x) and C87 (Δ). The ratios of the circle areas are equal to the *I*-band flux ratios from K93. Right: Flux ratios from C87 (Δ), K93 (x), S93 (□), and V86 (o).

MG 0414+0534 (B: 04<sup>h</sup>14<sup>m</sup>37.7321<sup>s</sup>, +05°34'44.270" [J2000; K93])

ID	$-\Delta\alpha$ "	$\Delta\delta$ "	Peak mJy/beam	$-\Delta\alpha$ "	$\Delta\delta$ "	$F_{5\text{GHz}}$ mJy	$-\Delta\alpha$ "	$\Delta\delta$ "	$I'$ mag
A1	-0.577	-1.945	185.9	-0.588	-1.934	401	-0.59	-1.94	20.07
	-0.594	-1.939	39.0						
A2	-0.712	-1.543	122.3	-0.721	-1.530	362	-0.75	-1.54	20.95
	-0.728	-1.516	28.7						
B	0.000	0.000	38.6	0.000	0.000	156	0.00	0.00	20.95
	-0.048	-0.023	13.8						
C	1.345	-1.454		1.361	-1.635	58	1.40	-1.69	21.83
G							0.42	-1.36	21.08
X?							0.98	-0.03	23.32

E95 data (left): 5GHz VLBI data, with A1, A2, and B resolved into two subcomponents each. Position uncertainties are 11-14 mas for A1 and A2, and 22 mas for B. The flux uncertainty is estimated to be 10-15 mJy/beam; in addition, the VLBI observations are thought to have resolved out the low surface brightness emission. The VLBI detection of C is probably spurious. Data from 1992 June 7.

K95 data (center): 5GHz VLA data. The uncertainties in the relative positions are 0.01". The uncertainties in the peak fluxes are ~ 4%. Data from Jan 1993.

S93 data (right): The position uncertainties are 0.01"-0.04". Magnitude uncertainties are 0.03-0.11, and 0.16 for X. Data from Hiltner 2.4m telescope, 1991 Nov 2-4.

References: A93 (Annis & Luppino, 1993, ApJL, 407, L69), E95 (Ellithorpe 1995, Ph.D. thesis, MIT), H92 (Hewitt et al., 1992, AJ, 104, 968), K93 (Katz & Hewitt 1993, ApJL, 409, L9), K95 (Katz et al., 1995, in preparation, given in E95), S93 (Schechter & Moore, 1993, AJ, 105, 1), and V95 (Vanderriest et al., these proceedings).

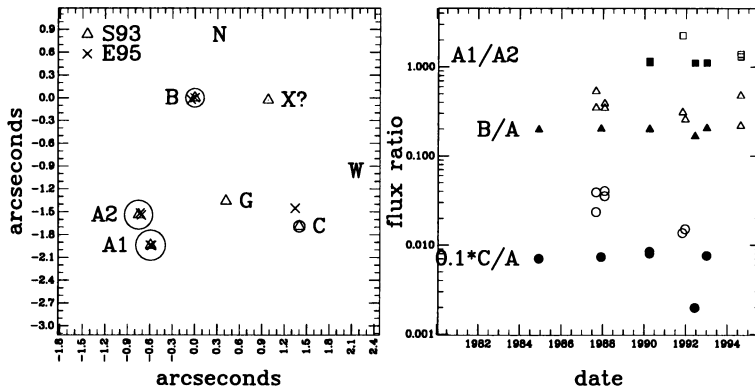


Figure 8. Left: Positions from E95 (x) and S93 (Δ). The ratios of the circle areas are equal to the flux ratios from K95. Right: Flux ratios A1/A2 (□), B/A (Δ), and C/A (o). Filled symbols denote radio data (H92, K93, E95, K95), while other symbols denote optical (H92, S93, V95) or infrared (A93) data.

CLASS 1608+656 (A:  $16^{\text{h}}09^{\text{m}}13.956^{\text{s}}$ ,  $+65^{\circ}32'28.97''$  [J2000; M95])

ID	$-\Delta\alpha$ "	$\Delta\delta$ "	Flux Ratio (8.4 GHz)
A	0.00	0.00	$2.06 \pm 0.06$
B	-0.74	-1.96	$\equiv 1.00$
C	-0.75	-0.46	$0.85 \pm 0.03$
D	1.13	-1.24	$0.26 \pm 0.03$
G	0.56	-1.16	

QSO images: The data for A, B, C, and D are from M95. The uncertainties in the positions are not stated. The flux of component B is  $17.80 \pm 0.44$  mJy; the total flux is  $73.2 \pm 0.9$  mJy. Data from VLA (A configuration), 8.4 GHz, 1994 Mar 1.

Galaxy: The data for G are from S95. The uncertainty in the position of the galaxy is correlated with the shape of the galaxy; it is estimated to be  $\sim 10$  mas. Data from Hiltner 2.4m telescope, Apr 1995.

Miscellaneous: (from M95) Optical observations from Palomar Observatory 5m telescope (1994 Aug 9) give magnitudes for the entire system (including lensing galaxy) of  $r = 19.4$ ,  $i = 19.2$ , uncertain by a few tenths of a magnitude. Observations with Keck 10m telescope (1994 Aug 22) indicate that in the  $K$ -band the flux of the lensing galaxy is  $\sim 4$  times greater than total flux from the 4 images, and that the galaxy image has an axial ratio of  $b/a = 0.56 \pm 0.10$  with its major axis having a position angle of  $60^\circ$ . (The galaxy is likely to be more elliptical, because the image is circularized by the seeing).

References: M95 (Myers et al., 1995, ApJL, 447, L5; also these proceedings), and S95 (Schechter, 1995, private communication).

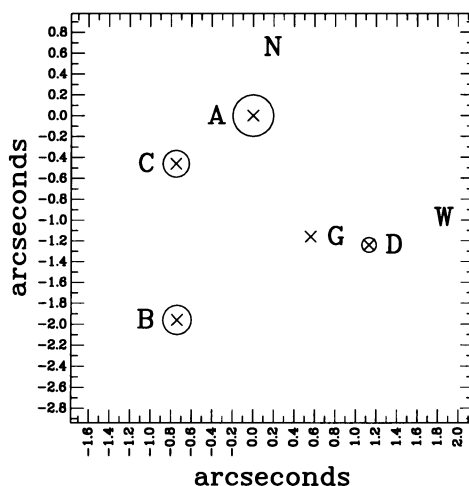


Figure 9. Positions from M95 (A, B, C, D) and S95 (G). The ratios of the circle areas are equal to the flux ratios from M95.

2237+0305 ( $22^{\text{h}}37^{\text{m}}57.3^{\text{s}}$ ,  $+03^{\circ}05'49''$  [B1950; Hu85])

ID	$-\Delta\alpha$ "	$\Delta\delta$ "	$g$ mag	$B$ mag	$-\Delta\alpha$ "	$\Delta\delta$ "	$R$ mag	$U$ mag	Peak $\mu\text{Jy}/\text{beam}$
A	0.000	0.000	17.74	17.96	0.000	0.000	17.42	16.63	65.5
B	0.672	1.673	17.60	17.82	0.676	1.686	17.29	16.53	64.2
C	-0.626	1.202	18.41	18.66	-0.625	1.200	18.11	17.56	26.5
D	0.854	0.517	18.62	18.98	0.869	0.520	18.34	17.97	59.4
G	0.093	0.936			0.083	0.918			

Cr91 data (left): The relative positions have a formal error of 5 mas, largely due to limitations in the correction for detector distortion. The magnitude of B is  $17.60 \pm 0.10$  in  $g$  (F502M), and  $17.82 \pm 0.07$  in  $B$  (F430W). The relative magnitudes have uncertainties of 0.05 mag for A and 0.10 mag for C and D. Data from HST FOC, 1990 Aug 27.

Ri92 data (center): The relative positions have an uncertainty of 15 mas. The relative magnitudes are accurate to  $\pm 0.04$  mag in  $R$  (F702W) and  $\pm 0.06$  mag in  $U$  (F336W). The  $R$  band was calibrated by comparing photometry of a star  $9''$  from the center of the galaxy with  $r$ -band measurements by Ra91; the  $U$  band was not calibrated, so  $U$  brightnesses are given in instrumental magnitudes, subject to an arbitrary zero point. Data from HST WFPC, 1990 Dec 18.

Fa95 data (right): The uncertainty in the peak fluxes is  $8.3 \mu\text{Jy}/\text{beam}$ . The total flux is  $336 \pm 60 \mu\text{Jy}$ . Data from 8 GHz VLA observations, 25 June 1995.

Miscellaneous: The central velocity dispersion of the galaxy is  $\sigma_p = 215 \pm 30$  km/s (Fo92). The bulge of the galaxy has a position angle  $\text{PA} = 68^\circ$  on the sky (Ri92).

References: Co91 (Corrigan et al., 1991, AJ, 102, 34), Cr91 (Crane et al., 1991, ApJL, 369, L59), Fa95 (Falco 1995, private communication), Fo92 (Foltz et al., 1992, ApJL, 386, L43), Ho94 (Houde & Racine, 1994, AJ, 107, 466), Hu85 (Huchra et al., 1985, AJ, 90, 691), N91 (Nadeau et al., 1991, ApJ, 376, 430), Ra91 (Racine, 1991, AJ, 102, 454), Ra92 (Racine, 1992, ApJL, 395, L65), Ri92 (Rix et al., 1992, AJ, 104, 959), and Y88 (Yee, 1988, AJ, 95, 1331).

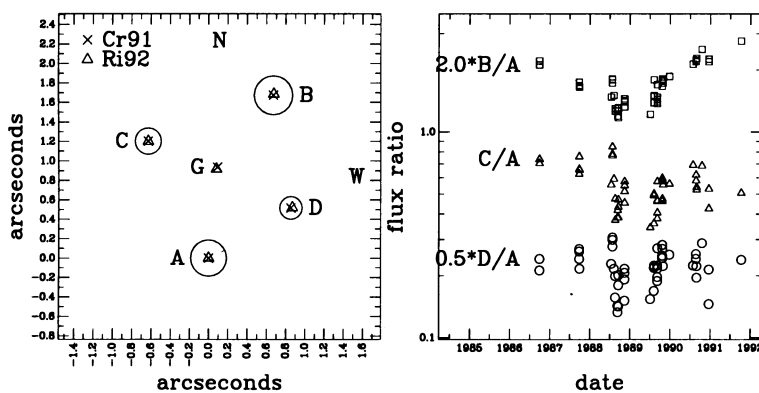


Figure 10. Left: Positions from Cr91 ( $\times$ ) and Ri92 ( $\Delta$ ). The ratios of the circle areas are equal to the  $B$ -band flux ratios from Cr91. Right: flux ratios from Ho94, which includes data reported originally in Co91, Cr91, N91, Ra91, Ra92, Ri92, and Y88.

B1422+231 (B:  $14^{\text{h}}24^{\text{m}}38.094^{\text{s}}$ ,  $+22^{\circ}56'00.59''$  [J2000; P92])

ID	$-\Delta\alpha$ "	$\Delta\delta$ "	$F_{5\text{GHz}}$ mJy	$F_{8.4\text{GHz}}$ mJy	$-\Delta\alpha$ "	$\Delta\delta$ "	$r$ mag	$g$ mag
A	-0.3908	0.3194	216	148	-0.39	0.32	16.77	16.92
B	0.0000	0.0000	221	153	0.00	0.00	16.45	16.64
C	0.3357	-0.7457	115	79	0.34	-0.77	17.25	17.44
D	-0.9449	-0.8059	4.5	3.9	-0.96	-0.80	20.40	20.56
G					-0.68	-0.58	21.8	> 22.4

P92 data (left): The relative positions are from the 5 GHz MERLIN map and are uncertain by a few mas. Data from 8.4 GHz VLA map, 1991 June 16, and from 5 GHz MERLIN map, 1991 Aug 31.

Y94 data (right): The relative positions have an uncertainty of  $0.01''$  for A, B, and C, and  $0.02''$  for D. The galaxy position has an uncertainty  $0.05''$ . The relative magnitudes have an uncertainty of  $\sim 0.02$  mag for A, B, and C, and  $\sim 0.1$  mag for D; the absolute magnitudes have a systematic uncertainty of 0.07 mag. Data from CFHT, 1993 Apr 26.

Miscellaneous: The lensing galaxy is observed with a redshift  $z_l = 0.647 \pm 0.001$  (Ha95). Two bright galaxies several arcseconds away from the lens are thought to perturb the lensing potential (Ha95, Ho94); the positions relative to B are as follows:

ID	$-\Delta\alpha$ (")	$\Delta\delta$ (")
G2	-9.0	-5.2
G3	-3.6	-7.3

References: A95 (Akujor et al., these proceedings), Ha95 (Hammer et al., 1995, A&A, 298, 737), Ho94 (Hogg & Blandford, 1994, MNRAS, 268, 889), L92 (Lawrence et al., 1992, MNRAS, 259, 5P), P92 (Patnaik et al., 1992, MNRAS, 259, 1P; also private communication), R93 (Remy et al., 1993, A&A, 278, L19), and Y94 (Yee & Ellingson, 1994, AJ, 107, 28).

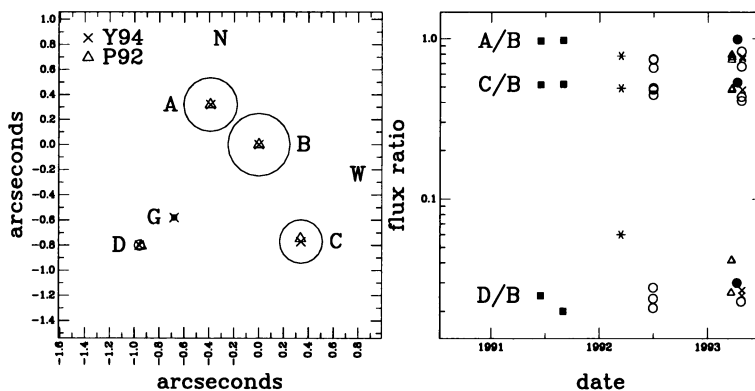


Figure 11. Left: Positions from Y94 ( $\times$ ) and P92 ( $\Delta$ ). The ratios of the circle areas are equal to the  $r$ -band flux ratios from Y94. Right: Flux ratios from L92 (\*), P92 ( $\blacksquare$ ), R93 ( $\Delta$ ), Y94 ( $\times$ ), and A95 ( $\circ$ ,  $\bullet$ ). Filled symbols denote radio data.

H 1413+117 ( $14^{\text{h}}13^{\text{m}}20.11^{\text{s}}$ ,  $+11^{\circ}43'37.8''$  [B1950; K90])

ID	$-\Delta\alpha$	$\Delta\delta$	Flux Ratio		
	"	"	<i>R</i>	<i>I</i>	<i>B</i>
A	0.000	0.000	1.00	1.00	1.00
B	-0.741	0.168	0.85	0.90	0.84
C	0.497	0.715	0.74	0.76	0.83
D	-0.351	1.046	0.61	0.59	0.61

S95 data (left): The uncertainty in the relative positions is about 4 mas, and the uncertainty in the alignment of the CCD is about  $0.1^{\circ}$ . Data from Hiltner 2.4m telescope, Apr 1992.

K90 data (right): The uncertainties in the flux ratios are not stated. The *R* magnitude for A is assumed to be 18.30. The system is detected at radio wavelengths, and the images have peak fluxes  $\sim 0.1 - 0.2$  mJy/beam. Optical data from Danish 1.54m telescope at ESO, 1988 Apr 27. Radio data from VLA (A configuration), 8.415 GHz, 1989 Jan 13.

References: A90 (Angonin et al., 1990, A&A, 233, L5), K90 (Kayser et al., 1990, ApJ, 364, 15), M88 (Magain et al., 1988, Nature, 334, 325), R95 (Remy et al., these proceedings), and S95 (Schechter, 1995, private communication).

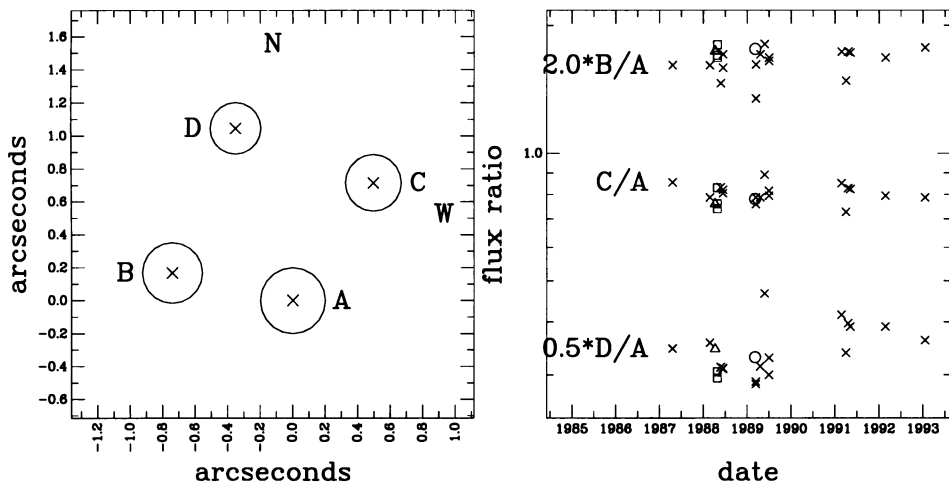


Figure 12. Left: Positions from S95. The ratios of the circle areas are equal to the *R*-band flux ratios from K90. Right: Flux ratios from A90 (o), K90 (□), M88 (Δ), and R95 (x).

HST 14176+5226 ( $14^{\text{h}}17^{\text{m}}36.3^{\text{s}}$ ,  $+52^{\circ}26'44''$  [J2000])

ID	$x$ "	$y$ "	$-\Delta\alpha$ "	$\Delta\delta$ "	$V$ mag	$I$ mag
A	-1.1	1.1	-1.31	-0.85	25.63	25.12
B	1.8	-0.4	0.77	1.68	25.77	25.38
C	1.0	1.2	-0.96	1.23	25.99	25.47
D	-0.3	-0.9	0.82	-0.48	25.97	25.55
G	0.0	0.0	0.00	0.00	21.68	19.71

R95 data: The  $(x, y)$  positions are in the HST observation frame, with the  $x$ -axis  $12.07^{\circ}$  clockwise from North; they were given (in R95) in units of WFC  $0.1''$  pixels. The  $(\Delta\alpha, \Delta\delta)$  positions were computed by rotating the  $(x, y)$  positions and retaining an extra digit. The position uncertainties are estimated to be about  $0.03''$ . The bands are  $V$  (F606W) and  $I$  (F814W). The magnitudes of the quasar images were computed using a  $0.3''$  square aperture and were corrected to total magnitudes assuming a point source; the magnitude uncertainties for components A, B, C, D (respectively) are 0.06, 0.07, 0.08, 0.08 in  $V$  and 0.10, 0.11, 0.13, 0.14 in  $V - I$ . The magnitude of the galaxy was determined by a fit to the light distribution; the magnitude uncertainties of the galaxy are 0.04 in  $V$  and 0.04 in  $V - I$ . Data from HST WFPC2, 1994 Mar 11.

References: R95 (Ratnatunga et al., these proceedings; also private communication).

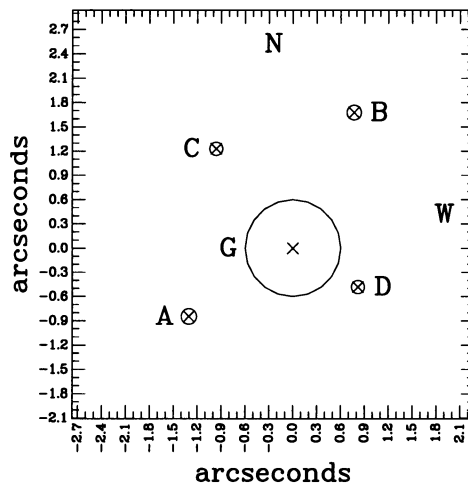


Figure 13. Positions from R95 ( $\times$ ). The ratios of the circle areas are equal to the  $V$ -band flux ratios.

HST 12531–2914 ( $12^{\text{h}}53^{\text{m}}06.7^{\text{s}}$ ,  $-29^{\circ}14'30''$  [J2000])

ID	$x$ "	$y$ "	$-\Delta\alpha$ "	$\Delta\delta$ "	$V$ mag	$I$ mag
A	-0.6	-0.2	0.62	0.12	27.02	26.77
B	0.6	0.3	-0.63	-0.22	26.89	26.46
C	-0.2	0.4	0.15	-0.42	26.72	26.38
D	0.3	-0.4	-0.25	0.43	27.51	26.69
G	0.0	0.0	0.00	0.00	23.77	21.82

R95 data: The  $(x, y)$  positions are in the HST observation frame, with the  $x$ -axis  $82.77^{\circ}$  counter-clockwise from North; they were given (in R95) in units of WFC  $0.1''$  pixels. The  $(\Delta\alpha, \Delta\delta)$  positions were computed by rotating the  $(x, y)$  positions and retaining an extra digit. The position uncertainties are estimated to be about  $0.03''$ . The bands are  $V$  (F606W) and  $I$  (F814W). The magnitudes of the quasar images were computed using a  $0.3''$  square aperture and were corrected to total magnitudes assuming a point source; the magnitude uncertainties for components A, B, C, D (respectively) are 0.15, 0.15, 0.11, 0.24 in  $V$  and 0.28, 0.23, 0.21, 0.34 in  $V - I$ . The magnitude of the galaxy was determined by a fit to the light distribution; the magnitude uncertainties of the galaxy are 0.06 in  $V$  and 0.07 in  $V - I$ . Data from HST WFPC2, 1995 Feb 15.

References: R95 (Ratnatunga et al., these proceedings; also private communication).

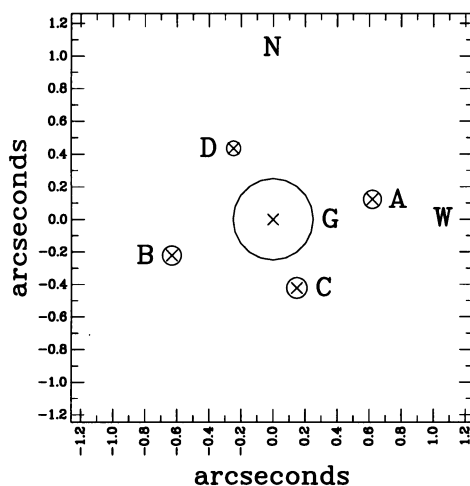
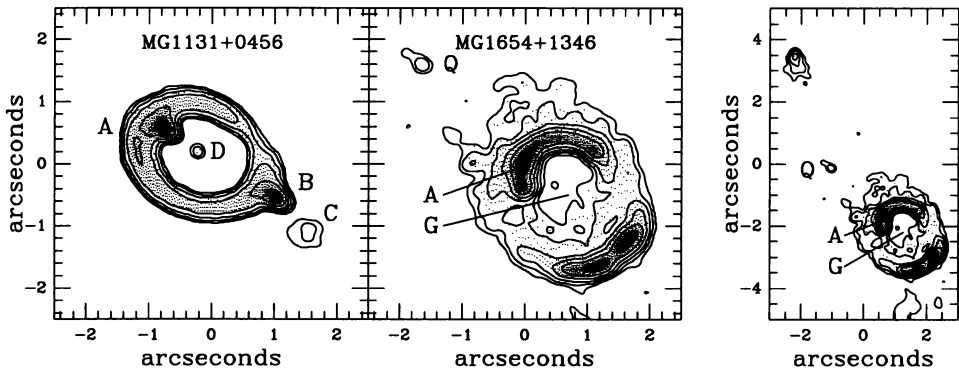


Figure 14. Positions from R95 ( $\times$ ). The ratios of the circle areas are equal to the  $V$ -band flux ratios.

## Extended-emission systems

Lens		RA	Dec	Flux
MG 1131+0456	A	$11^{\text{h}}31^{\text{m}}56.48^{\text{s}} \pm 0.1''$	$+04^{\circ}55'49.8'' \pm 0.1''$	$F_{15\text{GHz}}(\text{A}) = 3.18 \pm 0.10 \text{ mJy}$
	B-A	$-1.725'' \pm 0.010''$	$-1.087'' \pm 0.010''$	$F_{15\text{GHz}}(\text{B}) = 3.90 \pm 0.12 \text{ mJy}$
	D-A	$-0.4'' \pm 0.1''$	$-0.4'' \pm 0.1''$	$F_{8\text{GHz}}(\text{D}) = 0.32 \pm 0.06 \text{ mJy}$
	C-D	$-1.710'' \pm 0.010''$	$-1.299'' \pm 0.010''$	$F_{8\text{GHz}}(\text{C}) = 1.16 \pm 0.03 \text{ mJy}$ $F_{5\text{GHz}}(\text{total}) = 205 \text{ mJy}$
<p>Comments: Positions are J2000. Component A is resolved into two components, A1 and A2. The compact components A2 and B appear to be variable.</p> <p>References: Chen &amp; Hewitt, 1993, AJ, 106, 1719; Hewitt et al., 1995, AJ, 109, 1956.</p>				
MG 1654+1346	A	$16^{\text{h}}54^{\text{m}}41.83^{\text{s}}$	$+13^{\circ}46'22.0''$	
	G	$\Delta\alpha = -0.7''$	$\Delta\delta = -0.5''$	$m_r = 18.66 \pm 0.03$
	Q	$1.5''$	$1.3''$	$m_r = 20.93 \pm 0.03$
	Lensed Radio Lobe			$F_{5\text{GHz}} = 130.0 \text{ mJy}$
<p>Comments: Positions are J2000. Component A is a peak in the ring, but is not a compact component. The uncertainty in the absolute position of A is <math>0.1''</math>, and the uncertainty in the absolute positions of G and Q are <math>0.05''</math>. The quasar (Q) has <math>z = 1.74</math>, and the galaxy (G) has <math>z = 0.254</math>.</p> <p>References: Langston et al., 1989, AJ, 97, 1283; Langston et al., 1990, Nature, 344, 43.</p>				



**Figure 15.** Left: 8 GHz VLA map of MG 1131+0456. The contours are  $-2, 2, 4, 8, 16, 32, 64, 96\% \times 6.7 \text{ mJy}$ . The grayscale is linear. Right: 8 GHz VLA map of MG 1654+1346. The contours are  $-2, 2, 4, 8, 16, 32, 64, 96\% \times 4.7 \text{ mJy}$ . The grayscale is linear. Center: The lensed radio lobe of MG 1654+1346. The contours and grayscale are the same as in the full image. In all three images, the coordinate origin is arbitrary.

## Extended-emission systems

Lens	RA	Dec	Flux
B 1938+666			$F_{5\text{GHz}} = 316 \text{ mJy}$
References: Patnaik et al., 1993, Liège proceedings, p. 208.			
MG 1549+3047	G3 $15^{\text{h}}47^{\text{m}}12.56^{\text{s}}$	$+30^{\circ}56'18.0''$	$m_R = 23.3$
	G1 $\Delta\alpha = -6.62''$	$\Delta\delta = 3.39$	$m_R = 16.7$
	G2 $-2.48''$	1.78	$m_R = 20.5$
	Lensed Radio Lobe		$F_{5\text{GHz}} = 185 \text{ mJy}$
	Total		$F_{5\text{GHz}} = 257 \text{ mJy}$
<p>Comments: Positions are B1950. G3 is the quasar core, G1 is the lensing galaxy (<math>z = 0.111</math>), and G2 is probably a small galaxy associated with the lensing galaxy. The uncertainty in the absolute position of G3 is <math>0.3''</math>, and the uncertainty in the relative positions is <math>0.1''</math>; the magnitude uncertainties are 0.1 mag.</p> <p>References: Lehár et al., 1993, AJ, 105, 847, also private communication.</p>			

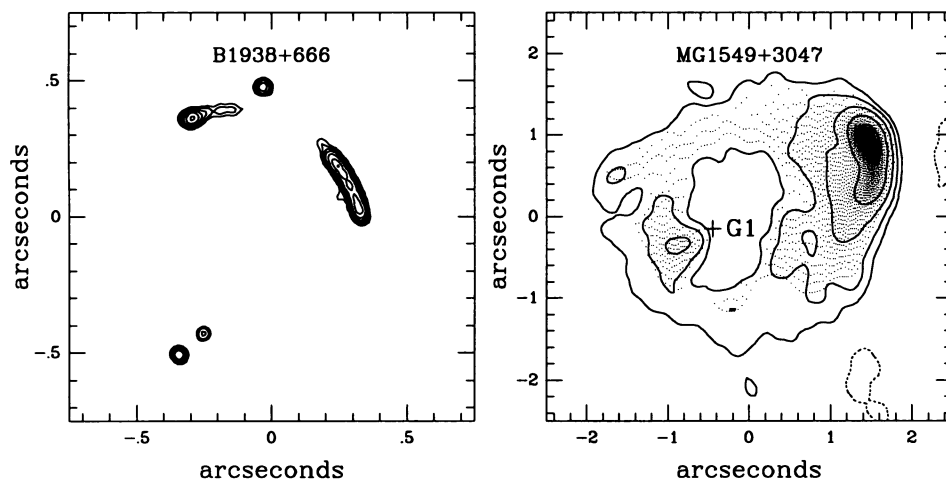


**Figure 16.** **Left:** 5 GHz MERLIN map of B 1938+666. The contours are  $-2, 2, 4, 8, 16, 32, 64, 96\% \times 36 \text{ mJy}$ . **Right:** 8.4 GHz VLA map of MG 1549+3047. The contours are  $-4, 4, 8, 16, 32, 64, 96\% \times 8.0 \text{ mJy}$ . The grayscale is linear. In both images, the coordinate origin is arbitrary.

Extended-emission systems

Lens	RA	Dec	Flux	
PKS 1830–211	A	18 <sup>h</sup> 33 <sup>m</sup> 39.94 <sup>s</sup>	–21°03′39.7″	$F_{2.3\text{GHz}}(\text{total}) \sim 10 \text{ Jy}$
	B	$\Delta\alpha = -0.7''$	$\Delta\delta = -0.7''$	$F_{8.4\text{GHz}}(\text{total}) \sim 8 \text{ Jy}$
<p>Comments: Positions are J2000, and the position uncertainty is 0.1". A and B are compact, bright sources; they sit on top of a low-level ring. A and B are highly variable (see, for example, Lovell et al.). There is evidence for scintillation as the light passes near the galactic center (Jones et al.).</p> <p>References: Jauncey et al., 1991, Nature, 352, 132; Jones et al., these proceedings; Lovell et al., these proceedings; Subrahmanyam et al., 1990, MNRAS, 246, 263; van Ommen et al., 1995, ApJ, 444, 561.</p>				
MG 0751+2716	$F_{5\text{GHz}} = 202 \text{ mJy}$			
<p>Comments: There are four components with mutual separations about 1". A magnitude ~19 galaxy with <math>z = 0.351</math> is probably the lensing galaxy.</p> <p>References: Lehar, 1993, Liège proceedings, p. 208, also private communication.</p>				

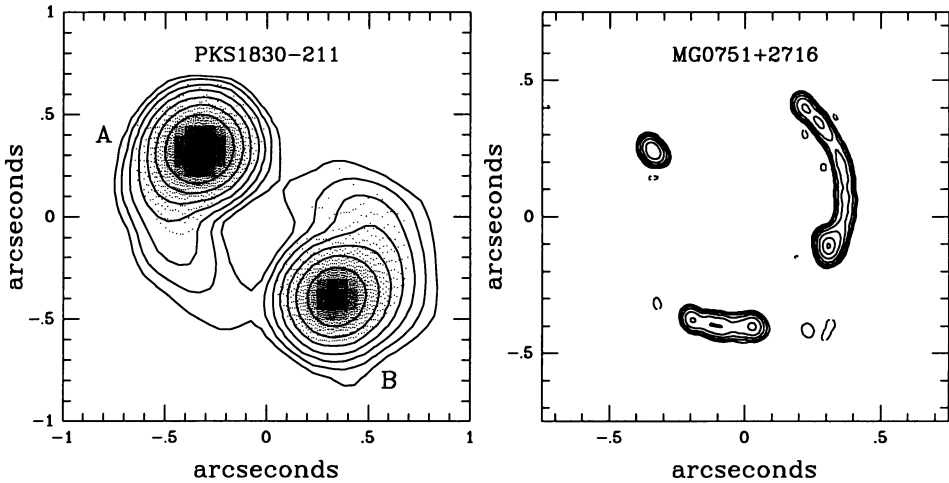
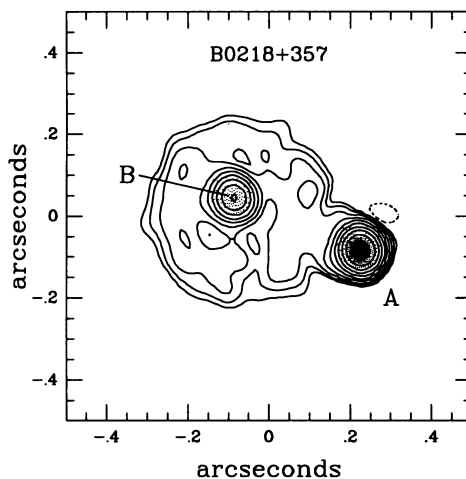


Figure 17. Left: 8 GHz VLA map of PKS 1830–211. The contours are –0.5, 0.5, 1, 2, 4, 8, 16, 32, 64, 96%  $\times 3.5 \text{ Jy}$ . The grayscale is linear. Right: 5 GHz MERLIN map of MG 0751+2716. The contours are –2, 2, 4, 8, 16, 32, 64, 96%  $\times 25 \text{ mJy}$ . In both images, the coordinate origin is arbitrary.

## Extended-emission systems

Lens		RA	Dec	Flux
B 0218+357	A1	02 <sup>h</sup> 21 <sup>m</sup> 5.483 <sup>s</sup>	+35°56'13.78"	$F_{15\text{GHz}}(\text{A1}) = 621 \pm 7 \text{ mJy}$
	A2–A1	1.07 mas	0.87 mas	$F_{15\text{GHz}}(\text{A2}) = 379 \pm 5 \text{ mJy}$
	B1–A1	309.2 mas	127.4 mas	$F_{15\text{GHz}}(\text{B1}) = 172 \pm 3 \text{ mJy}$
	B2–B1	1.47 mas	0.00 mas	$F_{15\text{GHz}}(\text{B2}) = 104 \pm 3 \text{ mJy}$
				$F_{5\text{GHz}}(\text{total}) = 1209 \text{ mJy}$

Comments: Positions are J2000. A and B are bright flat-spectrum compact components; the separation of the compact components and the diameter of the ring are 335 mas. The compact components A and B are resolved into two subcomponents each, with separations given above (from Pa95). These observations can be used to derive the magnification matrix (see Pa95, Po95). The bright components are variable, so that the flux ratio changes at the level of  $\sim 10\%$  (Pa93). The lens redshift of  $z_l = 0.6847$  is based on narrow emission and absorption lines (B93) and on HI emission (C93). A source redshift of  $z_s = 0.96$  is proposed based on a MgII emission line and associated absorption doublet (L95).  
References: B93 (Browne et al., 1993, MNRAS, 263, L32); C93 (Carilli & Rupen, 1993, ApJL, 412, L59); L95 (Lawrence, these proceedings); O92 (O'Dea et al., 1992, AJ, 104, 1320); Pa93 (Patnaik et al., 1993, MNRAS, 261, 435); Pa95 (Patnaik et al., 1995, MNRAS, 274, L5); Po95 (Porcas & Patnaik, these proceedings).



*Figure 18.* 5 GHz MERLIN map of B 0218+357. The contours are  $-0.125, 0.125, 0.25, 0.5, 1, 2, 4, 8, 16, 32, 64, 96\% \times 0.73 \text{ Jy}$ . The grayscale is linear. The coordinate origin is arbitrary.